WEBB INSTITUTE

November 18, 2016

Office of Naval Research

To Whom It May Concern:

SUBJECT: FINAL REPORTS

Enclose, please find the required final reports for ONR Grant N00014-14-1-0606 entitled "Partially Ventilated Transom Flow Elevations – Unsteady Analysis."

Please contact me with any questions or concerns relating to this submittal.

Sincerely

Richard A. Royce, Ph.D.
Director of Research
James J. Henry Professor of Naval Architecture
(516) 403-5932
rroyce@webb.edu

298 Crescent Beach Road
Glen Cove, New York 11542-1398
Telephone: 516-671-2213 · Fax: 516-674-9838
www.webb-institute.edu

REPORT DOCUMENTATION PAGE

Form Approved
OMB No. 0704-0188

1. REPORT DATE *(DD-MM-YYYY)*	2. REPORT TYPE	3. DATES COVERED *(From - To)*
30/06/2016	Final Technical Report	06/05/2014 - 30/06/2016

4. TITLE AND SUBTITLE
Partially Ventilated Transom Flow Elevations - Unsteady Analysis

5a. CONTRACT NUMBER
16PRO1802-00

5b. GRANT NUMBER
N00014-14-1-0606

5c. PROGRAM ELEMENT NUMBER

6. AUTHOR(S)
Richard A. Royce

5d. PROJECT NUMBER

5e. TASK NUMBER

5f. WORK UNIT NUMBER

7. PERFORMING ORGANIZATION NAME(S) AND ADDRESS(ES)
Webb Institute

8. PERFORMING ORGANIZATION REPORT NUMBER

9. SPONSORING/MONITORING AGENCY NAME(S) AND ADDRESS(ES)
ONR REG BOSTON N62879
495 SUMMER STREET ROOM 627
BOSTON, MA 02210-2109

10. SPONSOR/MONITOR'S ACRONYM(S)
ONR

11. SPONSOR/MONITOR'S REPORT NUMBER(S)

12. DISTRIBUTION/AVAILABILITY STATEMENT
DISTRIBUTION STATEMENT A. Approved for public release.

13. SUPPLEMENTARY NOTES

14. ABSTRACT
Prior research has investigated partially ventilated steady transom flows for a family of hulls that have a common fore-body with varying after-bodies. This project expands the investigation into unsteady transom flow elevations two of the five different transom configurations, including a round bilge and a deep-vee sections. A common wave profile was used for the experiments and wave elevations were measured at 24 different positions within the towing tank.. High definition video was used to capture the flow elevations for a range of speeds. This report presents the findings in terms of the transom Froude number and ventilation factors.

15. SUBJECT TERMS
Transom stern, ventilation, wave resistance, unsteady.

16. SECURITY CLASSIFICATION OF:			17. LIMITATION OF ABSTRACT	18. NUMBER OF PAGES	19a. NAME OF RESPONSIBLE PERSON
a. REPORT	b. ABSTRACT	c. THIS PAGE			Richard A. Royce
					19b. TELEPHONE NUMBER *(Include area code)*
U	U	U	UU		(516) 403-5932

Award Information

Award Number	N00014-14-1-0606
Title of Research	Partially Ventilated Transom Flow Elevations – Unsteady Analysis
Principal Investigators	Richard A. Royce Ph.D. and Adrian S. Onas, Ph.D.
Organization	Webb Institute

Technical Section

Technical Objectives

Transom sterns make prediction of ship's performance characteristics challenging, especially in the partially ventilated regime. Faster, medium fidelity potential flow codes such as the ones based on the Boundary Element Method (BEM) require a special treatment of the free surface boundary condition at the transom in order to correctly predict calm water resistance. Incident waves further complicate the flow kinematics around the vessel and possibly the characteristics of the transom flows, which become important when wave added resistance is considered. This research investigates the effect of incident waves on the stream wise discontinuity in hull geometry due to varying transom configurations ranging from round bilge to deep-vee sections. Transom flow wave elevations between the fully wetted and fully separated regimes are measured in waves and compared with the steady case for two different transoms. The effect of diffracted waves on the transom flow kinematics is analyzed experimentally and the data is used to validate high-fidelity unsteady fully-viscous CFD results from simulations performed in FINE™/Marine.

Technical Approach

Although transom sterns are ubiquitous in modern ship design, the hydrodynamics of vessels featuring a transom stern is not fully understood. The kinematics associated with the partially through fully ventilated flow at the stern are difficult to model using traditional potential flow approaches in calm water due to significant viscous effect involved at the transom, making it even more challenging when incident waves are present. The calm water problem has been studied extensively in the past half-century, beginning with St. Denis (1953), Saunders (1957) and Yeh (1965). More recently, theoretical and experimental work on transom sterns have been carried out by Scorpio and Beck (1997), Doctors (2006), Maki et al. (2004 and 2006), and Starke et al. (2007). There is very little information published on unsteady hydrodynamics of transom stern vessels. An attempt to tackle this problem theoretically and experimentally was made by Elangovan (2011). Transom sterns continue to be an attractive design feature on a variety of vessel types including recreational, commercial and naval craft. Aside from the obvious benefits given by increased space below deck and a more robust propulsion machinery arrangement, there are advantages associated with reduced calm water resistance, particularly for high-speed vessels operating above $Fn = 0.30$ (O'Dea et al., 1981).

Currently, the research effort has been to combine experimental and high fidelity numerical hydrodynamics (using fully viscous CFD codes) in order to address the problem more fundamentally, by reformulating the nonlinear free surface boundary condition at the stern through the use of wave elevation regression from transom elevations and wave pattern analysis. This way, the transom stern problem could potentially be made amenable to a more robust, inexpensive, and relatively accurate medium fidelity nonlinear potential flow approach. Experimental work in calm water supporting this methodology was reported by Royce et al (2015), where the effect of transom geometry on the transom Froude number was investigated.

In order to determine the complete effect that transom stern geometry has on partially ventilated flow, we need to study the impact of the incident wave field on transom stern hydrodynamics. The problem can be described using a potential flow decomposition of the total wave field created around the vessel moving with a constant velocity U in incident waves of circular frequency, ω. For brevity, suppose the vessel is moving in deep water, in a head sea harmonic incident wave system where radiation forces are neglected. Then, the total velocity potential becomes:

$$\Phi = Ux + \phi_S(x,y,z) + \phi_0(x,y,z)e^{i\omega t} + \phi_7(x,y,z)e^{i\omega t} \quad (1)$$

Here ϕ_S is the steady velocity potential of the Kelvin wake, $\phi_0 e^{i\omega t}$ and $\phi_7 e^{i\omega t}$ are the 1st harmonics of the unsteady velocity potentials of the incident and diffracted wave system, respectively. Removal of the radiation velocity potential makes it easier to isolate the diffraction component and it is achieved in practice by creating a fixed sinkage and trim experimental setup.
The total wave elevation recorded by a wave probe placed at a fixed location in the towing tank can also be decomposed in the corresponding constituents shown in Eq. (1), as follows:

$$\zeta(x,y,t) = \zeta_S(x,y) + \zeta_0(x,y)e^{i\omega t} + \zeta_7(x,y)e^{i\omega t} \quad (2)$$

Here the ζ_S is the amplitude of the steady wave system due to vessel forward motion creating the Kelvin wake, ζ_0 is the amplitude of the incident regular wave field and ζ_7 is the 1st order harmonic of the diffracted wave, respectively. In a vessel's fixed frame of reference, say amidships, we can express the total wave elevation in terms of the steady Kelvin wake and the 1st and 2nd order harmonics of the diffraction wave, at different transverse locations measured from the model's centerline:

$$\zeta_j(y,t) = \zeta_S(x,y) + \zeta_{7,1}(x,y)e^{i(\omega_e t')} + \zeta_{7,2}(x,y)e^{i(2\omega_e t')} \quad (3)$$

Here ζ_S is once again the amplitude of the steady wave system (including higher order terms), $\zeta_{7,1}$ is the amplitude of the 1st order diffracted wave and $\zeta_{7,2}$ is the corresponding amplitude of the 2nd order component. Note that the time varying wave elevation are a function of the wave encounter frequency, ω_e, while $t' = t + \frac{X_j}{U}$. It was shown by Ohkusu and Wen (1997) that an adequate wave pattern and therefore the amplitude of the diffracted wave can be obtained using a series of wave probes fixed in the towing tank at X_j ($j = 1\ to\ N$), by performing a least-square fit of Eq. (3) to the measured wave elevation recorded by minimum 6 wave probes, adopted at a time interval Δt given by:

$$\Delta t = \frac{\Delta x}{U} = \frac{2\pi}{N\omega_e}, \quad (4)$$

where Δx is the longitudinal spacing between the wave probes and $N \geq 6$ is the number of wave probes.

TEST CONDITIONS

This section provides details of the models tested, the turbulence stimulation, the test instruments used, and the test matrices. This series of tests included a range of speeds in calm water and regular waves, which were limited only to Transom #1 and #5. Both models were tested at a common displacement of 11.34 kg (25.0 lbf). The models were towed in a fixed condition (for sinkage and trim) at the appropriate drafts for the common displacement.

Model Data

The model components were designed and built by Navatek, LTD, a partner in this research effort. The models were machined out of roughly 19 mm (0.75 in) thick PBHT-20 tooling board. The models were sealed with epoxy resin, painted safety yellow, and marked for waterlines and buttocks on the transom.

Turbulence Stimulation

Hama strips were used for turbulence stimulation on the hull. Four strips of electrical tape with a combined thickness of 0.028 inches were used for the Hama strips on the hull. The strips on the hull were cut to make a series of triangles that were roughly 3/4" on each side. The notches of the triangles were aligned at a distance of 3.75" aft of the stem. No correction was made for the hull turbulence stimulation in accordance with the findings of Hadler et. al. (2001).

Two different models have been investigated denoted here as T1 and T5, respectively. The models have an identical forebody and different afterbodies, which can be easily interchanged. The principal dimensions for model T1 and T5 are shown in Table 1 and Table 2, respectively. Note that model T1 is a round bilge and model T5 is a deep-vee, considered here as being representative for most modern transom stern designs. In addition, the different shapes attempt to better capture the changes in the effect of diffraction on the ventilation transom Froude number as well as the diffraction amplitude.

Table 1 Principal Dimensions of Model T1

LOA	66.14" (168 cm)	T	2.51" (6.4 cm)
LWL	60.21" (152.9 cm)	T_T	1.16" (2.9 cm)
B	8.99" (22.8 cm)	A_W	3.84 ft^2 (3567 cm^2)
D	8.51" (21.6 cm)	A_T	7.42 in^2 (47.9 cm^2)
Δ	25 lbf (11.34 kg)	LCF	-25.47" (-64.7 cm)

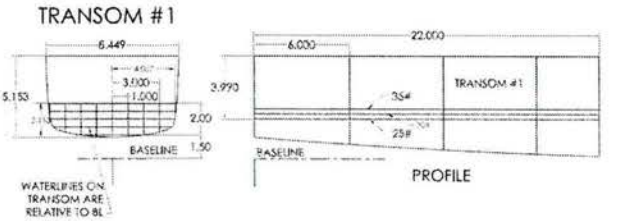

Fig. 1 Transom #1 striping and dimensions with grid used to Measure wave elevations (dimensions shown in inches, displacement in lbf)

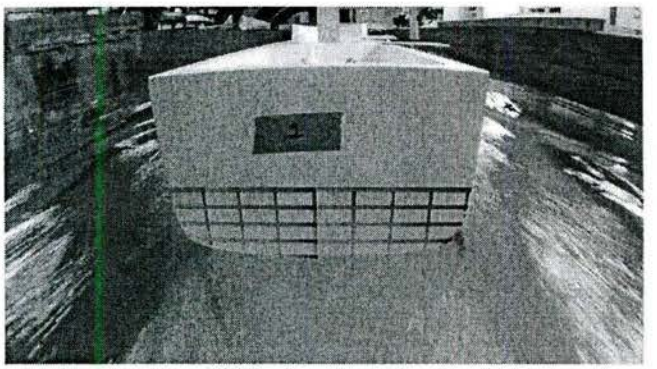

Fig. 2 Transom #1 during unsteady experiment

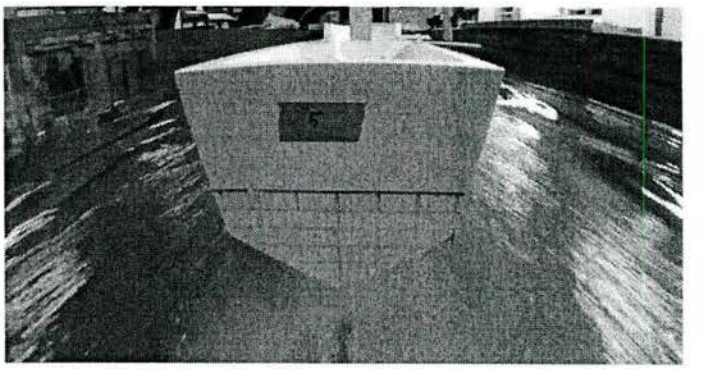

Fig. 3 Transom #5 during unsteady experiment

Table 2 Principal Dimensions of Model T5

LOA	66.14" (168.0 cm)	T	2.55" (6.5 cm)
LWL	60.25" (153.0 cm)	T_T	2.06" (5.2 cm)
B	9.01" (22.9 cm)	A_W	3.77 ft^2 (3502 cm^2)
D	8.51" (21.6 cm)	A_T	7.26 in^2 (46.8 cm^2)
Δ	25 lbf (11.34 kg)	LCF	-26.27" (-66.7 cm)

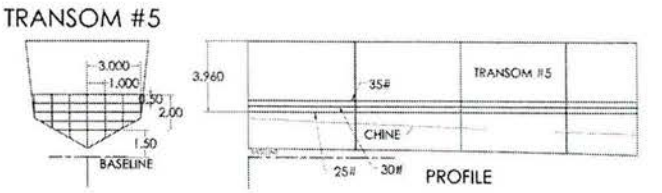

Fig. 4 Transom #5 striping and dimensions with grid used to measure wave elevations (dimensions shown in inches, displacement in lbf)

Photos of transoms for model T1 and T5 are shown in Fig. 2 and Fig. 3, respectively. The grid shown in Fig. 1 and Fig. 4 as well as the aforementioned photos, have been used to measure the transom wave elevation at the stern. The technique is explained in detail in the Test Instruments section.

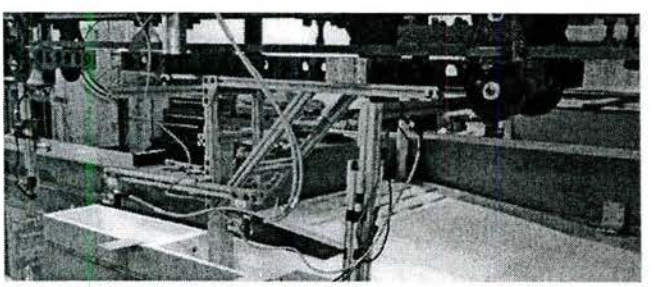

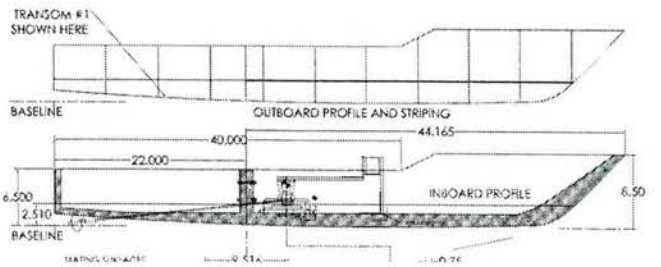

Fig. 5 Model T1 in towing carriage with lasers and wave probe on starboard side and camera behind the transom

Fig. 6 Construction details of ship model (dimensions in inches)

Test Instruments

The instruments were calibrated separately for each test condition. All data was sampled at 200 Hz and a tare was recorded for all instruments prior to each data run. The instruments were also calibrated after testing and the gain used for each set of tests was the average of the pre and post calibrations. LabView software was used to record the data and to make time averaged measurements of the data. The instrumentation attached to the model carriage, the two vertical laser probes and a wave probe are shown in Fig. 5.

Sinkage and Trim

Although both models were fixed in sinkage and trim, the residual heaving and pitching motions were measured using Micro-Epsilon optoNCDT laser triangulation displacement sensors, model ILD1302-200. These devices were placed symmetrically about the pivot point for the model (before restraint). The distance between lasers was 0.508 m (20in). The manufacturer indicates a full scale error of 0.05% or 0.1 mm (.004 in). During the unsteady experiments, the maximum pitching motion was in the order of 0.1°, whereas the heaving motions was almost undetectable.

Wave Probes

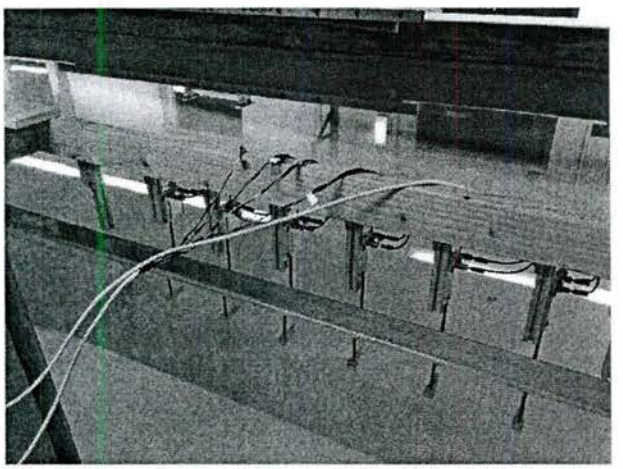

Fig. 7 Photo of wave probe array fixed in the tank side

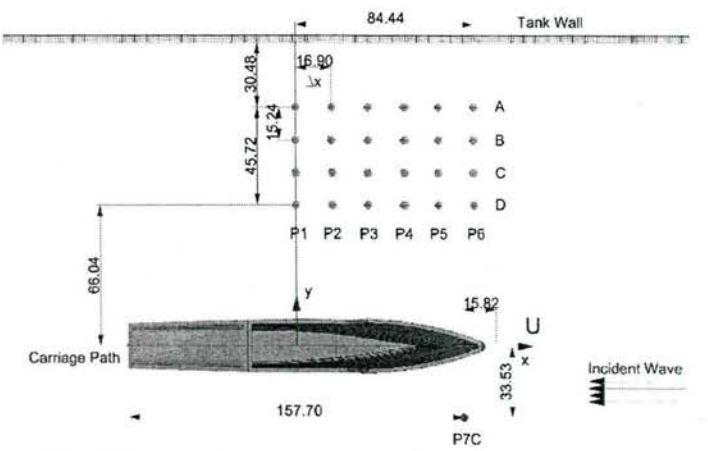

Fig. 8 Wave probe arrangement (dimensions in cm)

A 6-wave probe array was manufactured using the parts utilized in the calm water transom wave elevation measurements. As before, each of the wave probes consisted of two wires, as shown in Fig. 7. An additional wave probe was added in order to have enough wave records and allow a least-squares fit to be performed on Eq. (3). A sensitivity analysis was carried out by Elangovan (2011) who showed that the least-square fit of the wave record does not improve significantly when the wave probe number is doubled. Therefore, as a starting point, the minimum number of 6-wave probes was used for the entire unsteady test matrix. The wave probe array arrangement proposed to capture the wave pattern is shown in Fig. 8 and are denoted P1 through P6. These so-called Eulerian wave probes are fixed to

the tank wall and can be moved into 4 separate transverse configurations named A through D. The model wave probe is fixed to the carriage and is denoted as P7C. The coordinate system is shown in the vessel's fixed frame of reference and the incident regular waves are propagating toward the model from head seas direction.

The test matrix was designed to capture the wave elevation at the transom and the wave elevation at the model's wave probe (fixed to the towing carriage) and the static wave probe array with a sampling frequency of 200 Hz. A single incident regular wave was used of amplitude of $\zeta_a = 1.18\ cm$ and linear frequency $f = 0.813\ Hz$ ($\omega = 5.11 \frac{rad}{s}$). The wave steepness was 0.01 and the towing carriage speed varied from Fn =0.15 to 0.46, as shown in Tables 3 and 4 for models T1 and T5, respectively. The non-dimensional reduced frequency number defined in Eq. (6) below was maintained above 0.25 for all speed conditions in order to ensure that upstream wave propagation due to model disturbance is mitigated:

$$\tau = \frac{U\omega_e}{g} > 0.25 \tag{6}$$

Here U is the steady-state towing carriage velocity, ω_e is the wave encounter circular frequency and g is acceleration due to gravity. Note that transom based Froude number is the only parameter that varies between the two models due to the corresponding different drafts at the same tested displacement.

Table 3 Test matrix for Model T1

Diffraction Seakeeping Testing (Fixed Heave and Trim), Model T1																
λ/L	T	f	N	λ	H/λ	ζa		Ft	Fn	Intended Carriage Speed	ω.	T.	ΔX	ΔX	Array Length	τ
--	s	Hz	prb	in	--	in	cm	--	--	ft/s	rad/s	s	ft	in	in	--
1.4	1.23	0.813	6	92.59	0.01	0.46	1.18	1.10	0.15	1.94	6.70	0.94	0.30	3.64	18.20	0.40
								1.40	0.19	2.47	7.13	0.88	0.36	4.35	21.76	0.55
								1.70	0.24	3.00	7.56	0.83	0.42	4.98	24.92	0.70
								2.00	0.28	3.53	7.99	0.79	0.46	5.55	27.73	0.88
								2.30	0.32	4.06	8.42	0.75	0.50	6.05	30.26	1.06
								2.70	0.37	4.76	9.00	0.70	0.55	6.65	33.24	1.33
								3.00	0.42	5.29	9.43	0.67	0.59	7.05	35.26	1.55
								3.30	0.46	5.82	9.86	0.64	0.62	7.42	37.09	1.78

Table 4 Test matrix for Model T5

Diffraction Seakeeping Testing (Fixed Heave and Trim), Model T5																
λ/L	T	f	N	λ	H/λ	ζa		Ft	Fn	Intended Carriage Speed	ω.	T.	ΔX	ΔX	Array Length	τ
--	s	Hz	prb	in	--	in	cm	--	--	ft/s	rad/s	s	ft	in	in	--
1.4	1.23	0.813	6	92.59	0.01	0.46	1.18	0.83	0.15	1.94	6.70	0.94	0.30	3.64	18.20	0.40
								1.05	0.19	2.47	7.13	0.88	0.36	4.35	21.76	0.55
								1.28	0.24	3.00	7.56	0.83	0.42	4.98	24.92	0.70
								1.50	0.28	3.53	7.99	0.79	0.46	5.55	27.73	0.88
								1.73	0.32	4.06	8.42	0.75	0.50	6.05	30.26	1.06
								2.03	0.37	4.76	9.00	0.70	0.55	6.65	33.24	1.33
								2.25	0.42	5.29	9.43	0.67	0.59	7.05	35.26	1.55
								2.48	0.46	5.82	9.86	0.64	0.62	7.42	37.09	1.78

Video Recording

The measurement technique proposed by Royce et al (2015) has been used, which in this research was enhanced by performing a digital post-processing using the open source GNU Image Manipulation Program (GIMP). Similar to the calm water test procedure, the gridding on the transom was the aid in visual identification of the transom flow elevations. Videos and still images of the transom have been taken using and HD camera Replay XD Prime X 16.0 as shown in Fig. 8. In order to account for distortions, an additional transformation and mapping of the actual distances on the transom to monitor distances, were created for the two transom models at the same displacement of 25 lbf.

Fig. 8 Wave probe arrangement (dimensions in cm)

Results

Ventilation Factors

The ventilation factors from the CFD results are compared to the towing tank measurements and in general, they show good agreement. The time averaged ventilation factors calculated from the maxima and minima free surface elevations for Transom 1 at two locations are shown in Fig. 9 and 10 for centerline and ¼ breadth buttock, respectively. The ventilation factor was calculated as follows:

$$V(F_T) = \frac{T_T - T_W(F_T)}{T_T} \tag{7}$$

where $T_W(F_T)$ is the local wetted draft measured at the transom stern and T_T is the static transom draft.

The vessel's transom based Froude number is given by:

$$F_T = \frac{U}{\sqrt{gT_T}} \tag{5}$$

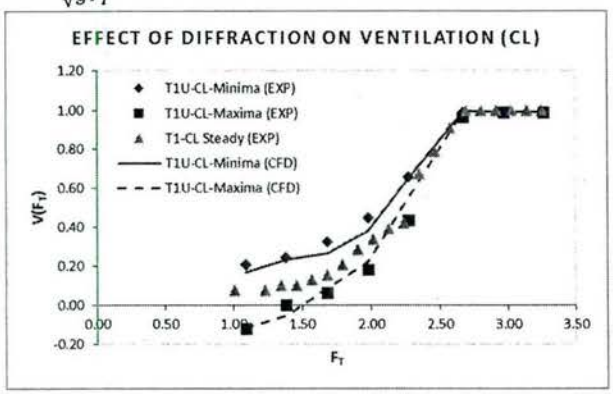

Fig. 9. Transom ventilation at CL (T1)

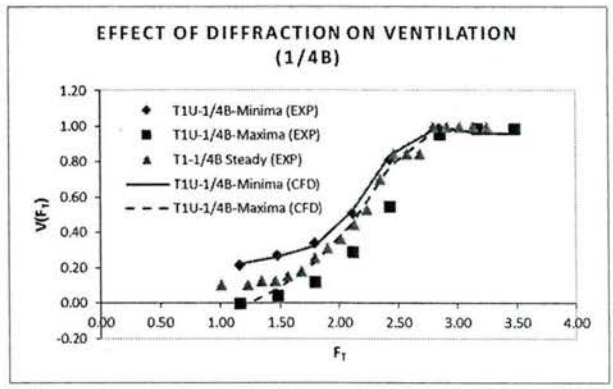

Fig. 10 Transom ventilation at 1/4 breadth buttock (T1)

Through the speed regime where the transom is transitioning from wet to dry, the tow tank experiments show a larger range of ventilation factor than the CFD results, with the difference more pronounced in the maxima, especially for the ¼ breadth buttock, as seen in Fig. 10. The steady ventilation factors from previous experiments carried out by Royce et al (2015) have also been integrated in the plot for comparison. As expected, for the most part, the steady result falls approximately in the middle or as an average between the maxima and minima, which would indicate that incident wave and/or diffraction do not have a significant effect on the ventilation factor. However, when carefully comparing the minima and maxima of the unsteady transom measurements with the steady component, there is an indication of an effect from the incident waves on the ventilation factor especially on the quarter breadth buttock. It is the opinion of the authors that such effect cannot be fully ascertained using the imaging method only. Rather, the use of a higher fidelity experimental approach is needed to accurately measure the wave elevation such as LiDAR, a type of acoustic system placed on the bottom of the towing tank or attach the wave probes directly to the transom.

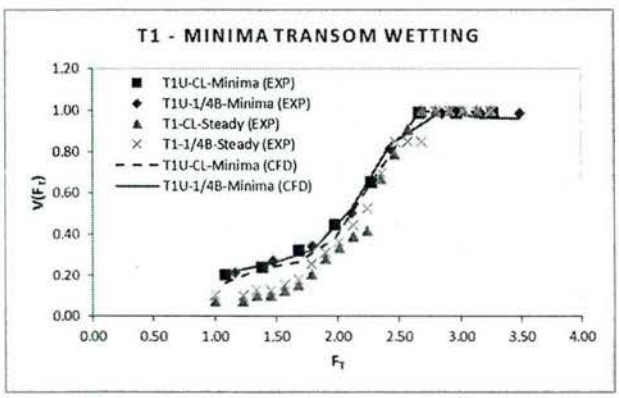

Fig. 11 Transom minima at CL and ¼ breadth buttock

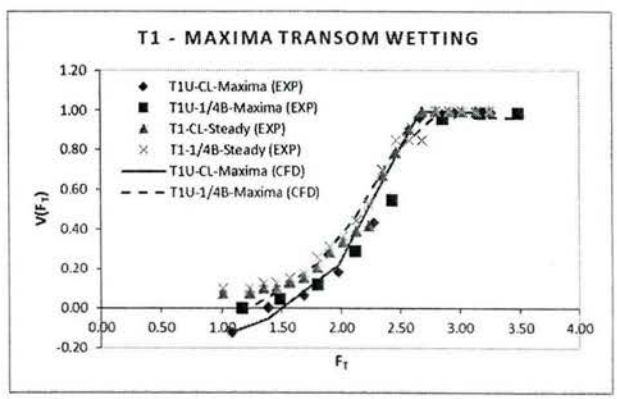

Fig. 12. Transom maxima at CL and ¼ breadth buttock

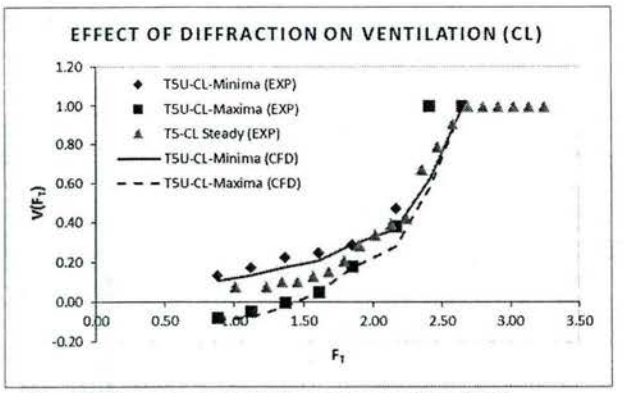

Fig. 13 Transom ventilation at centerline (T5)

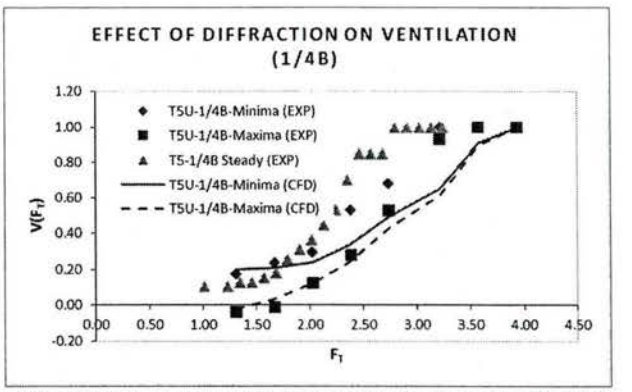

Fig. 14 Transom ventilation at ¼ breadth buttock (T5)

We now compare the experimental results with the CFD analysis carried out in incident regular waves with Model T5. There seems to be a divergence between the steady and the average unsteady results on the quarter breadth buttock at $F_T \cong 1.75$, which is clearly shown in Fig. 14. This is effect is clearly visible from very low values of transom Froude number with great divergence from the mean for the rest of the partially ventilated regime.

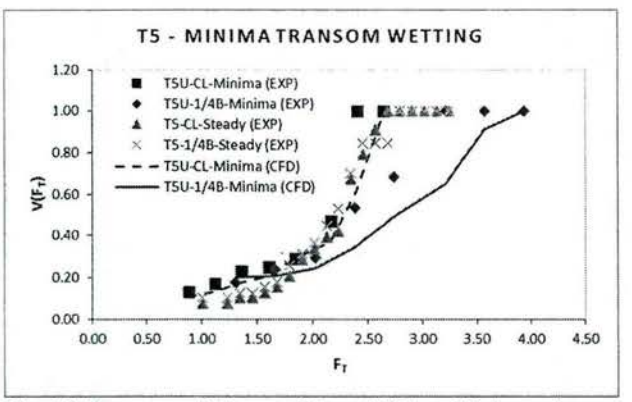

Fig. 15 Transom minima at CL and ¼ breadth buttock

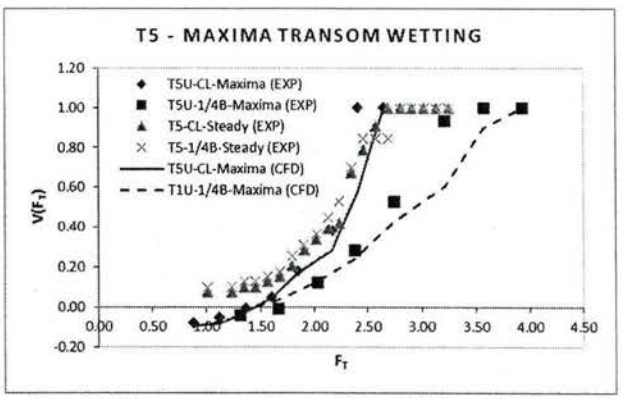

Fig. 16. Transom maxima at CL and ¼ breadth buttock

A similar but less pronounced behavior of such divergence between steady and unsteady ventilation is observed in Fig. 13 for the centerline result, but at a much higher value of $F_T \cong 2.25$. There is reasonable agreement between the experimental and the CFD solution through the partially ventilated regime, with poorer agreement for the quarter breadth buttock, especially for the lower transom wave elevations denoted here as minimas. This effect is better seen in Fig. 15, which compares only the lower transom wave elevation values together with the steady results for Model T5.

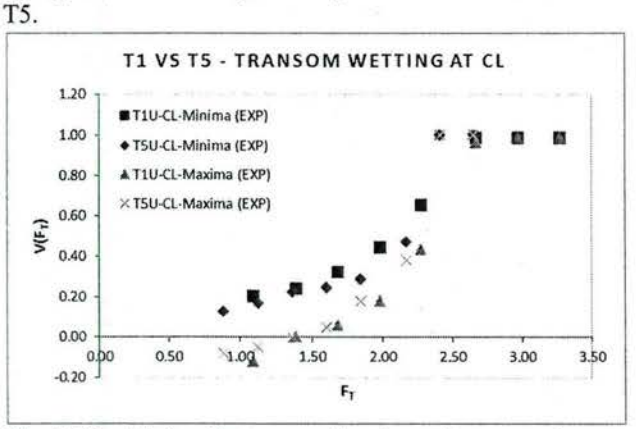

Fig. 17 Ventilation factor as a function of transom shape

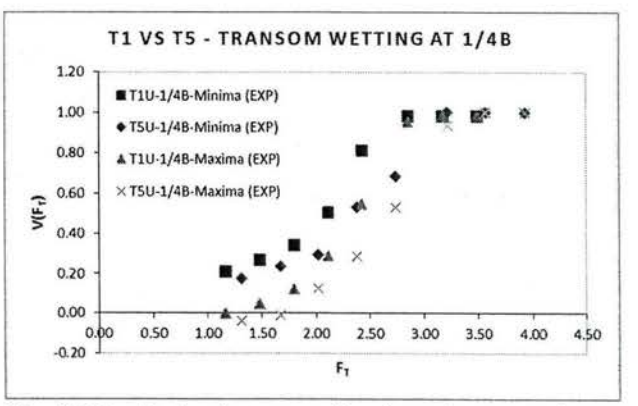

Fig. 18 Ventilation factor as a function of transom shape

In Fig. 17 we compare the results between the lower and higher values of the unsteady transom wave elevations by examining the ventilation factor as a function of transom shape.

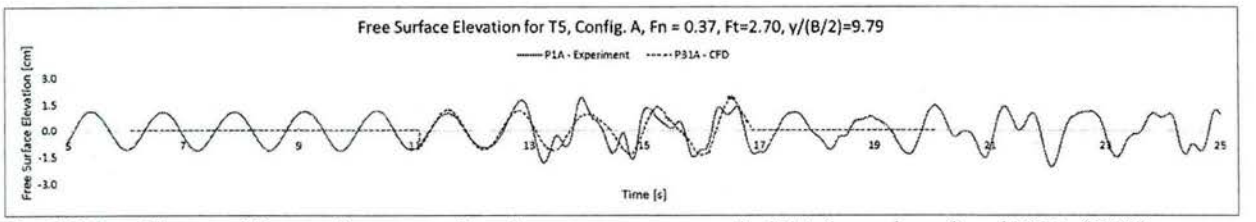

Fig. 19 Time history of free surface wave elevation at wave array probe P1A (experiment) and P31A (CFD)

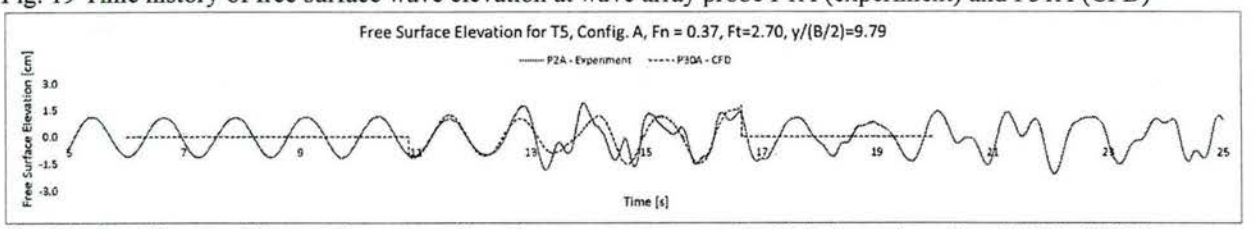

Fig. 20 Time history of free surface wave elevation at wave array probe P2A (experiment) and P30A (CFD)

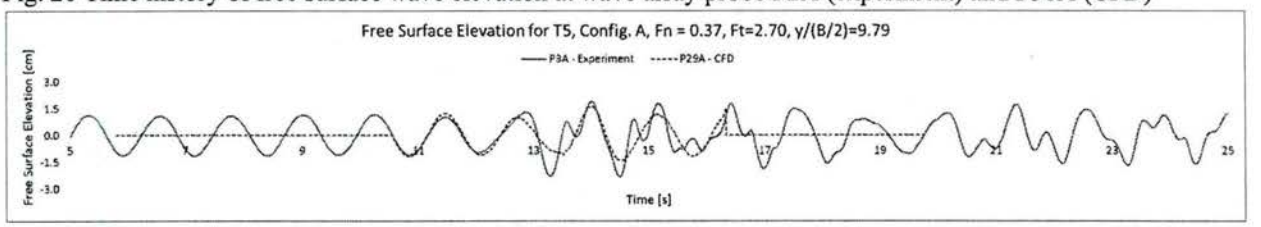

Fig. 21 Time history of free surface wave elevation at wave array probe P3A (experiment) and P29A (CFD)

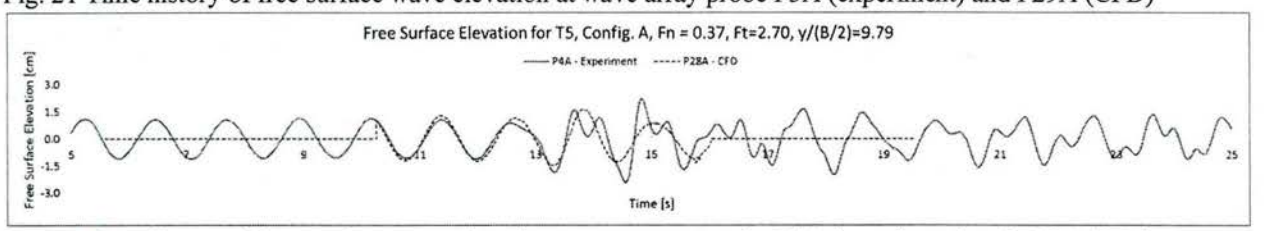

Fig. 22 Time history of free surface wave elevation at wave array probe P4A (experiment) and P28A (CFD)

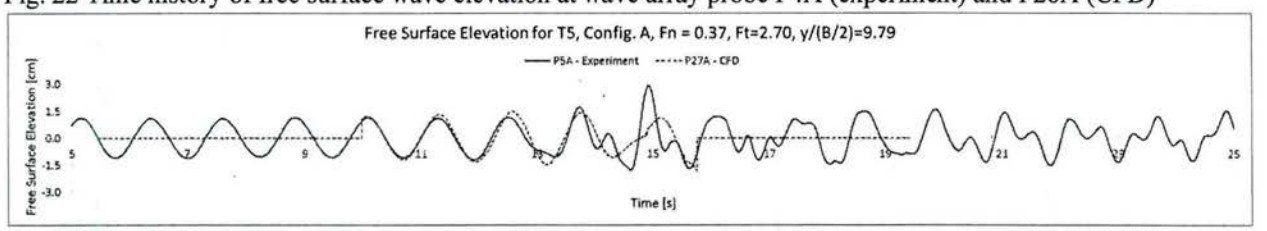

Fig. 23 Time history of free surface wave elevation at wave array probe P5A (experiment) and P27A (CFD)

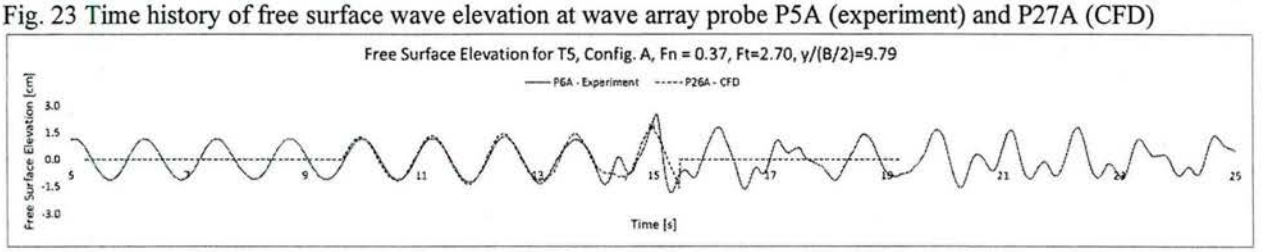

Fig. 24 Time history of free surface wave elevation at wave array probe P6A (experiment) and P26A (CFD)

The incident waves will affect the transom wave elevation differently for most range of the partially ventilated regime. A direct comparison is made between the time histories of the wave probe free surface elevation recorded during the experiment and the CFD simulations for Configuration A of the wave array, which corresponds to transverse line

parallel to the CL of the model at y/(B/2) =9.79. In general, as shown in Fig. 19-24, there is good agreement between experiment and CFD. The numerical solution does not capture well the region of interaction between the incident wave, Kelvin wake and first and higher order harmonics of the diffracted wave.

REGRESSION ANALYSIS

One of the main difficulty is separating the constituents of the total free surface wave elevation recorded by the wave probes. A fully nonlinear treatment of the diffracted wave generated by the moving model is more adequate to characterize the wave system, which has not been attempted in this paper.

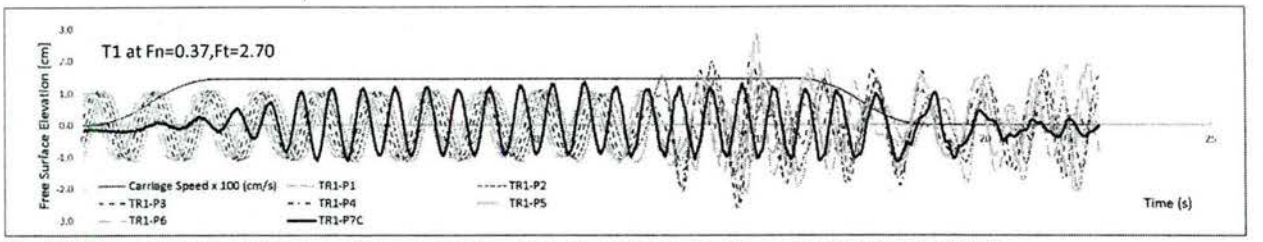

Fig. 28 Time histories of free surface wave elevation for all wave probes at y/(B/2) = 9.79; T1

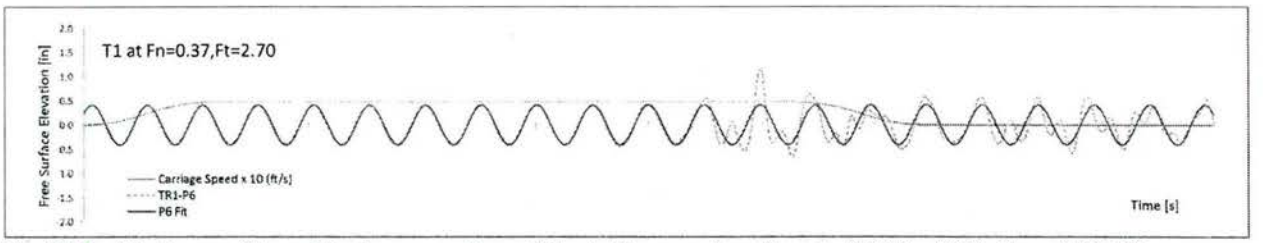

Fig. 29 Incident wave fit used in decomposition of the total wave elevation at y/(B/2) = 9.79, Fn = 0.37; T1

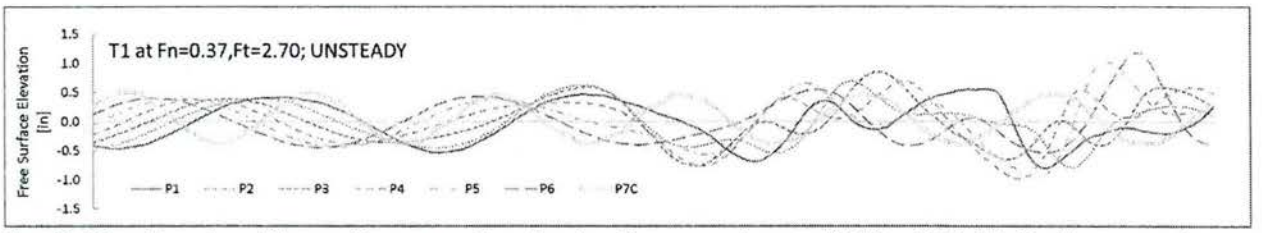

Fig. 30 Time histories of free surface wave elevation for all wave probes at y/(B/2) = 9.79; T1 (incident waves)

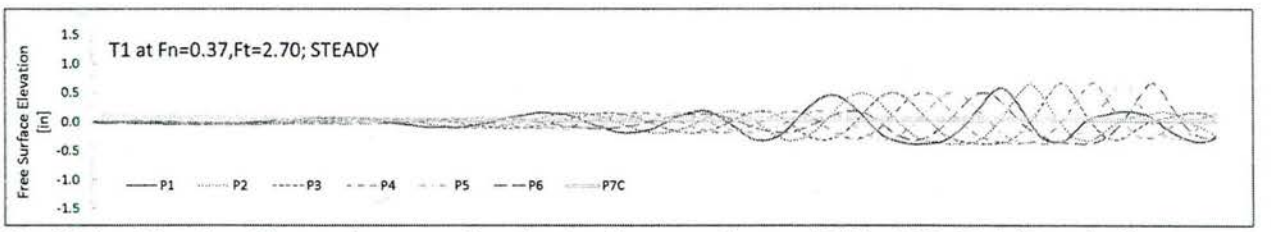

Fig. 31 Time histories of free surface wave elevation for all wave probes at y/(B/2) = 9.79; T1 (without incident waves)

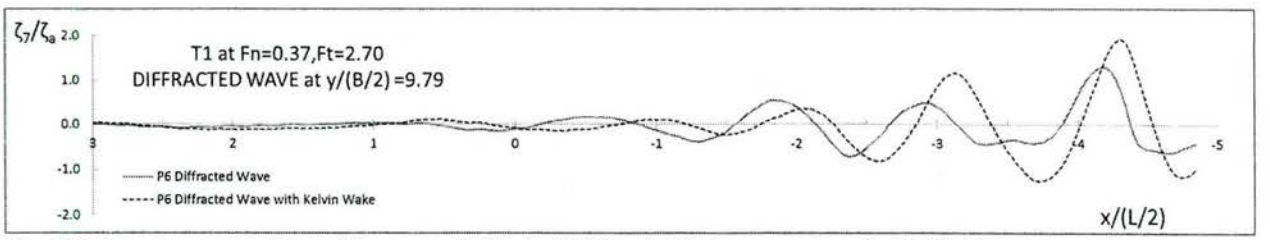

Fig. 32 Linear decomposition of the wave field at y/(B/2) = 9.79 along a range of x/(L/2); T1

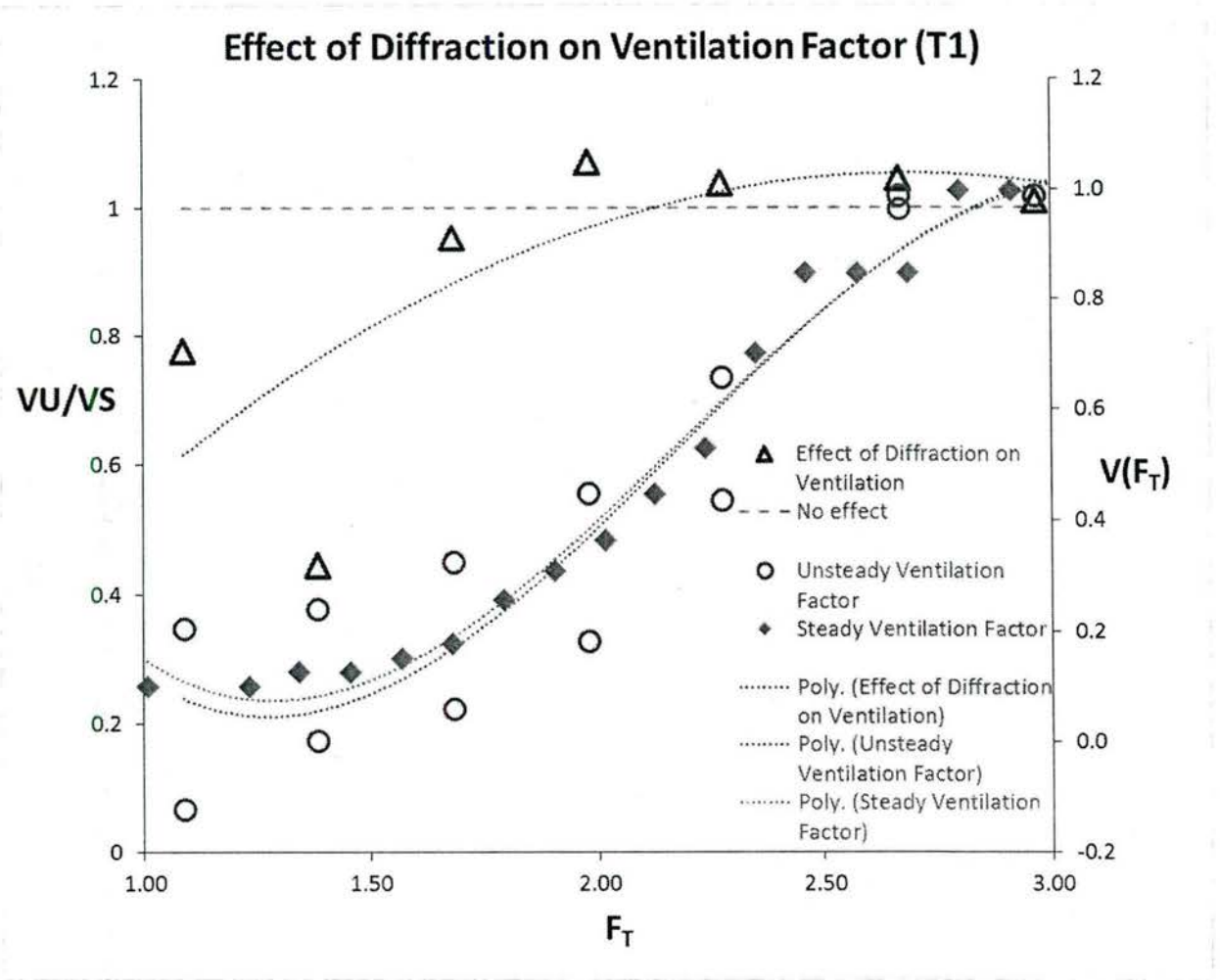

Fig. 33 Higher order fit of steady and unsteady ventilation

As a starting point, we used a quasi-linear approach to describe the constituents of the total wave elevation starting with the first order harmonics of the incident wave and Kelvin wake and the diffracted component, as shown at the introductory section in Eq. (2). The results are shown in Fig. 28-32. Since the incident wave cannot be adequately measured using the carriage wave probe when other wave systems are scattered, as seen in Fig. 28 and even before the interaction (note the nonlinearities in the peaks and troughs), a regular wave fit was generated and adopted in the decomposition of the total wave elevation (Fig. 29). Since the transverse location is the furthest from the model for Configuration A with y/(B/2) = 9.79, the majority of the wave record contains mostly the incident wave. This procedure can be applied at different transverse locations to generate a complete wave pattern provided a regression analysis is carried out using a least squares fit to the free surface elevation readings using a higher order model. The preliminary results are confirming that the measurement technique is adequate for a regression analysis using the experimental data obtained from the wave probe array.

To better quantify the effect of diffraction on transom stern ventilation, higher order polynomials were fit to the unsteady minima and maxima and the steady ventilation factors results. In Fig. 33, VU/VS represents the ratio of unsteady to steady ventilation factors. Since the precision uncertainty is not included in this plot, it is difficult to ascertain with confidence the impact of diffraction on the ventilation factor. However, as a qualitative analysis we can conclude that in steady conditions the transom ventilates slightly faster compared to the incident wave case, especially for lower value of transom Froude number of around 2.25. It appears that well within the partially ventilated regime, and around F_T=2.3, the steady and unsteady ventilation fits cross-each other, with the effect of diffraction on ventilation becoming more significant and all the way through the fully ventilated regime. This becomes clear when

we examine the values of $VU/VS > 1$ as a function of F_T, indicating that diffraction may increase the ventilation factors in incident waves.

Conclusion

The unsteady component of this research examined the effect of incident waves on the partially ventilated transom flows using an experimental and numerical approach. The main objective was to determine if incident waves affect the ventilation factor when compared to the steady runs for two different transom stern configurations, a round bilge (T1) and a deep-vee (T5). It was found that the latter transom shape has a less pronounced (or abrupt) ventilation profile in the unsteady condition compared to the steady case, especially for the quarter breadth buttock. However, since the transom wave elevations were measured using a low fidelity image processing technique, we could not yet establish the accuracy of this difference. The second objective was to ascertain if the wave system can be measured in the vicinity of the model such that a wave pattern can be generated and the diffracted wave elevation be separated from the total wave elevation using a least squares fit technique. It was found that the measuring technique works and that CFD simulations agree generally well with the experimental measurements. The third objective was twofold: to determine if RANS simulations using FINE™/Marine are adequate in predicting free surface wave elevations at the transom and around the moving vessel in incident waves, which was satisfied in general through reasonable agreement in the validation results; and if a higher order regression analysis can be carried out from the validated numerical data to further develop a mathematical model of the free surface at the transom, which needs further development.

Progress Statement Summary

This grant was approved in May of 2014. A test matrix was developed in the January of 2015 and the wave probe array was manufactured in the summer of 2015. A series of steady and unsteady tests were carried out in February of 2016. Several difficulties were encountered during the spring of 2016 tests. The model setup was not stiff enough to provide an effective fixed in sinkage and trim arrangement. A modification was made to the towing carriage assembly and the tests were repeated in March – April 2016. The heaving and pitching motions were reduced but still not found satisfactory.

The two forced block measuring the heaving force and trimming moment were removed and additional stiffening and reinforcement was provide in the towing carriage assembly. A series of trials were conducted in June 2016 concluding that the new heave staff connected to the model created an acceptable fixed in sinkage and trim arrangement. The steady experiments covering only transom#1 and #5 have been completed at the end of June 2016 and part of July 2016. Capturing the data visually was a time consuming task, often requiring several viewings of each video to determine the appropriate wetted transom draft. In order to estimate the uncertainty in the data capturing methods, the data was captured twice and the results were compared to make the uncertainty estimate. The work is being reported at the 2016 SNAME Annual Meeting in Seattle, WA.

Over the period of the grant, Webb requested, and was granted two separate no-cost extensions for this project. The original completion date was set for 15 July 2015 and the final completion date was 30 June 2016. The project is complete and the results will be presented in a SNAME Annual Meeting paper entitled "Unsteady Behavior of Partially-Ventilated Transom Flows in Waves"

Webb was awarded another grant for work related to this project, N00014-16-1-2964. That project will carry this effort into further seakeeping analysis and the development of experimental methogologies.

Bibliography

Doctors, L.J. "Hydrodynamics of the Flow Behind a Transom Stern." Proceedings 29st Israel Conference on Mechanical Engineering, Haifa, Israel, May 2003.

Doctors, L.J. "Influence of the Transom-Hollow Length on Wave Resistance." 21st International Workshop on Water Waves and Floating Bodies, Loughborough, UK, April 2006.

Elangovan, M. "Seakeeping of High Speed Ships with Transom Stern and the Validation Method with Unsteady Waves around Ships", Ph.D. Dissertation, Hiroshima University, Hiroshima, Japan, 2011.

Hadler, J.B., Gallagher, N.J., VanHoof, R.W., and the Webb Institute Class of 2002. "Model Resistance Testing in the Robinson Towing Tank at Webb Institute." Proceeding of the 26th ATTC, Glen Cove, NY, July 2001.

Kring, D.C., Milewski, W.M., and Fine, N.E. "Validation of a NURBS-Based BEM for multihull ship seakeeping", 25th Symposium on Naval Hydrodynamics, St. John's, Newfoundland and Labrador, Canada, 2004.

Kring, D., Keipper, T., Rosenthal, B., Szlatenyi, C., and Datla, R. "Transom Stern Modeling and Validation Through Ventilation Transition Speeds." 2013 Gran Challenges on Modeling and Simulation Conference, Toronto, Canada, 2013.

Maki, K.J., Troesch, A.W., and Beck, R.F. "Qualitative Investigation of Transom Stern Flow Ventilation." 19th International Workshop on Water Waves and Floating Bodies, Cortona, Italy, March 2004.

Maki, K.J., Doctors, L.J., Beck, R.F., and Troesch, A.W. "Transom-Stern Flow for High-Speed Craft." FAST 2005, St. Petersburg, Russia, June 2005.

Maki, K.J., Iafrati, A., Rhee, S., Beck, R.F. and Troesch A.W. "The Transom-Stern Modeled as a Backward Facing Step." 26th Symposium on Naval Hydrodynamics, Rome, Italy, September 2006.

O'Dea, J., Jenkins, D., and Nagle, T. "Flow Characteristics of a Transom Stern Ship." Technical Report, David W. Taylor Naval Ship Research and Development Center DTNSRDC-81/057, September 1981.

Ohkusu, M. and Wen, G. "Radiation and Diffraction Waves of a Ship at Forward Speed". Proceedings of the Twenty-First Symposium on Naval Hydrodynamics, Trondheim, Norway, 1996.

Royce, R. and Doherty, P. "Transom Flow Elevations in the Partially Ventilated Condition", Proceedings of the 13th International Conference on Fast Sea Transportation (FAST), Washington, D.C., 2015.

St. Denis, M., "On the Transom Stern." Marine Engineering, Volume 58:7 (1953): 53-54.

Saunders, H. (Ed.) Hydrodynamics in Ship Design, Society of Naval Architects and Marine Engineers, Volume 1 (1957): 326.

Scorpio, S.M., Beck, R.F. "Two-Dimensional Inviscid Transom Stern Flow." 12th International Workshop on Water Waves and Floating Bodies, France, 1997.

Starke, B., Raven, H., and van der Ploeg, A. "Computation of Transom-Stern Flows Using a Steady Free-Surface Fitting RANS Method." 9th International Conference on Numerical Ship Hydrodynamics, Ann Arbor, Michigan August 2007.This grant was approved in the summer of 2013. The model selection and development took place during the late